Journal of Power Sources 196 (2011) 5027–5034

Contents lists available at ScienceDirect

Journal of Power Sources

journal homepage: www.elsevier.com/locate/jpowsour

The interaction of biomass gasification syngas components with tar in a solid oxide fuel cell and operational conditions to mitigate carbon deposition on nickel-gadolinium doped ceria anodes

J. Mermelstein [a], M. Millan [a], N.P. Brandon [b,*]

[a] Chemical Engineering, Imperial College London, SW7 2AZ, United Kingdom
[b] Earth Science Engineering, Imperial College London, RSM Building, London SW7 2AZ, United Kingdom

ARTICLE INFO

Article history:
Received 26 October 2010
Received in revised form 26 January 2011
Accepted 2 February 2011
Available online 12 February 2011

Keywords:
Biomass
Gasification
Tars
SOFC
Carbon

ABSTRACT

The combination of biomass gasification with solid oxide fuel cells (SOFCs) is gaining increasing interest as an efficient and environmentally benign method of producing electricity and heat. However, tars in the gas stream arising from the gasification of biomass material can deposit carbon on the SOFC anode, having detrimental effects to the life cycle and operational characteristics of the fuel cell. This work examines the impact of biomass gasification syngas components combined with benzene as a model tar, on carbon formation on Ni/CGO (gadolinium-doped ceria) SOFC anodes. Thermodynamic calculations suggest that SOFCs operating at temperatures > 750 °C are not susceptible to carbon deposition from a typical biomass gasification syngas containing 15 g m^{-3} benzene.

However, intermediate temperature SOFCs operating at temperatures < 650 °C require threshold current densities well above what is technologically achievable to inhibit the effects of carbon deposition. SOFC anodes have been shown to withstand tar levels of 2–15 g m^{-3} benzene at 765 °C for 3 h at a current density of 300 mA cm^{-2}, with negligible impact on the electrochemical performance of the anode. Furthermore, no carbon could be detected on the anode at this current density when benzene levels were <5 g m^{-3}.

1. Introduction

The formation of carbon deposits on SOFC anodes can lead to severe anode degradation and irreversible damage [1]. Carbon formation from tar species can be minimized by anode morphology, and operating parameters such as steam and current density [2]. However the impact of H_2, CO_2, CO, and CH_4 combined with tar in the gas stream on SOFC anodes is not well understood. CO and CH_4 present in the syngas can be directly oxidized as fuel in the SOFC, though hydrogen oxidation is kinetically favoured. However CO and CH_4 can form carbon by CO disproportionation and CH_4 decomposition under thermodynamically favourable operating conditions of low O/C ratios. CO_2, as well as steam, can have a positive impact on decreasing the amount of carbon deposition through reforming reactions, discussed further in the following.

1.1. Internal reforming of syngas species

The high operating temperatures of SOFCs and catalytic activity of nickel based anodes make them ideal for direct internal reforming of hydrocarbon based fuels. Carbon formation can occur however, deactivating the catalyst, and reducing fuel cell performance if the O/C ratio is too low.

Steam and CO_2 are commonly used to reform hydrocarbons to H_2 and CO. Reforming of methane (Eq. (1)) and other hydrocarbon based fuels, such as benzene in this study (Eq. (2)), utilizing CO_2 occurs through the following reactions:

$$CH_4 + CO_2 \leftrightarrow 2CO + 2H_2 \quad \Delta H^{298}_{rxn} = 247 \text{ kJ mol}^{-1} \tag{1}$$

$$C_6H_6 + 6CO_2 \leftrightarrow 12CO + 3H_2 \quad \Delta H^{298}_{rxn} = 952 \text{ kJ mol}^{-1} \tag{2}$$

and by steam reforming in Eqs. (3) and (4):

$$CH_4 + H_2O \leftrightarrow CO + 3H_2 \quad \Delta H^{298}_{rxn} = 206 \text{ kJ mol}^{-1} \tag{3}$$

$$C_6H_6 + 6H_2O \leftrightarrow 6CO + 6H_2 \quad \Delta H^{298}_{rxn} = 705 \text{ kJ mol}^{-1} \tag{4}$$

There are several side reactions that could result in carbon deposition on the fuel cell anode. Carbon formation can occur via the decomposition of carbonaceous fuel such as CH_4 and C_6H_6 (Eq. (5)) and from the reverse Boudouard reaction (Eq. (6)).

$$CxH_y \leftrightarrow xC + \frac{y}{2}H_2 \tag{5}$$

$$2CO \leftrightarrow C + CO_2 \quad \Delta H^{298}_{rxn} = -173 \text{ kJ mol}^{-1} \tag{6}$$

* Corresponding author. Tel.: +44 20 7594 5704; fax: +44 20 7594 7444.
E-mail address: n.brandon@imperial.ac.uk (N.P. Brandon).

0378-7753/$ – see front matter © 2011 Elsevier B.V. All rights reserved.
doi:10.1016/j.jpowsour.2011.02.011

Methane decomposition is favoured at high temperatures, whereas the Boudouard reaction is favoured at lower temperatures ($T < 650\,^{\circ}C$) approaching that of intermediate temperature SOFCs [3–5]. The production of H_2 and CO can be affected by the reverse water gas shift (RWGS) reaction (Eq. (7)), methanation (Eq. (8)), and steam reforming (Eq. (3)) from the production of water in Eqs. (7) and (8), which will compete with CO_2 reforming, affecting the H_2/CO ratio [6].

$$CO_2 + H_2 \leftrightarrow CO + H_2O \quad \Delta H_{rxn}^{298} = 41.2\,kJ\ mol^{-1} \tag{7}$$

$$CO_2 + 4H_2 \leftrightarrow CH_4 + 2H_2O \quad \Delta H_{rxn}^{298} = -164.9\,kJ\ mol^{-1} \tag{8}$$

These side reactions become important in understanding the mechanism of tar reforming at the anode of SOFCs by the addition of CO_2 and steam, when these are used to suppress carbon formation.

The deactivation of catalysts and active sites within a SOFC anode cermet by carbon deposition is of great concern when reforming hydrocarbon based fuels. Carbon formation has been found to be more severe with dry reforming, particularly because of the low H/C ratios found in the feed gas [7–9]. Dry reforming between 700 and 850 °C can lead to vermicular whisker carbon and graphitic platelets [10], which are more tightly bound and harder to remove from the catalyst.

An increase in the current density within the SOFC corresponds to an increase in oxygen ion transport across the electrolyte from the cathode to anode. This allows several key reforming and electrochemical oxidation reactions to take place at the anode under load, as shown below:

$$H_2 + O^{2-} \leftrightarrow H_2O + 2e^- \quad \Delta H_{rxn}^{298} = -242\,kJ\ mol^{-1} \tag{9}$$

$$CO + O^{2-} \leftrightarrow CO_2 + 2e^- \quad \Delta H_{rxn}^{298} = -283\,kJ\ mol^{-1} \tag{10}$$

$$C + O^{2-} \leftrightarrow CO + 2e^- \quad \Delta H_{rxn}^{298} = -111\,kJ\ mol^{-1} \tag{11}$$

$$C + 2O^{2-} \leftrightarrow CO_2 + 4e^- \quad \Delta H_{rxn}^{298} = -394\,kJ\ mol^{-1} \tag{12}$$

$$CH_4 + O^{2-} \leftrightarrow CO + 2H_2 + 2e^- \quad \Delta H_{rxn}^{298} = -37\,kJ\ mol^{-1} \tag{13}$$

$$C_6H_6 + 15O^{2-} \leftrightarrow 6CO_2 + 3H_2O + 30e^- \quad \Delta H_{rxn}^{298} = -3170\,kJ\ mol^{-1} \tag{14}$$

It is suggested by Moon and Ryu [11] that the electrochemical oxidation reactions (9) and (10) are faster than the dry reforming reaction (1). This suggests that CO and H_2 are produced through the reforming of CH_4 and used to produce electricity through the electrochemical oxidation reactions (9) and (10) [11,12], while the electrochemical oxidation of methane (13) is not likely to occur unless the ratio of $CH_4/CO_2 \gg 1$ [12]. In the case of tar utilization in this study, the tar to oxidant level is $\ll 1$, such that the increase in performance of the fuel cell anode, as implied above, would not be attributed to direct oxidation of the tar, but rather to the direct oxidation of CO and H_2 produced through internal reforming of the tar at the anode.

Nonetheless, the interaction of tar species with syngas species (H_2, CO_2, CO, CH_4), CH_4 decomposition, and CO disproportionation can lead to significant carbon deposition, causing deterioration of the anode [1]. Increased current density results in a higher flux of oxygen ions to be transferred from cathode to anode, allowing for increased partial oxidation of carbon (Eqs. (11) and (12)) [2,12–14]. Partial oxidation of carbonaceous species is most efficient above the threshold current density, at which carbon formation is no longer thermodynamically predicted [2,15,16].

1.2. Interaction of steam and CO_2 reforming

One of the major problems in the reforming of hydrocarbon based fuels with CO_2 is the rapid rate in which carbon formation occurs with low steam content [17,18]. In the case of CO_2 methane reforming, carbon deposition is drastically reduced when steam and CO_2 reforming are carried out simultaneously [17]. However it is known that the adsorption of CO_2 competes with the adsorption of steam and hydrocarbons involved with steam reforming, inhibiting the overall steam reforming reaction [19,20], which may affect the steam reforming of tars in the gas stream.

Tars and hydrocarbon species undergo catalytic decomposition [21–23] at the operating temperature of SOFCs. Inhibition of this mechanism from sufficiently high CO_2 adsorption on the catalyst could lead to gas phase pyrolysis of tar and other hydrocarbons in the syngas, catalyzed by steam [24,25], and carbon formation by free radical gas phase condensation reactions [26] that could additionally lead to the growth of higher molecular weight polyaromatic hydrocarbons (PAHs) that condense on the catalyst as amorphous char type carbon, discussed in Refs. [27,28]. It is therefore important to understand the interaction of each of the syngas components with tar to determine their effect on carbon formation and fuel cell operation. This study looks at the subsequent addition of each of the syngas components, H_2, CO_2, CO, and CH_4, on carbon formation on Ni/CGO powder and Ni/CGO anodes operating at 765 °C at open circuit and under load. Thermodynamic predictions are compared with experimental results to suggest operational parameters such as syngas composition, temperature, and current density to suppress the formation of carbon when fuel cells are exposed to syngas containing tar.

2. Experimental

2.1. Experimental set-up

A SOFC test station using 2 types of experiments has been developed to test the carbon deposition characteristics of synthetically generated biomass gasification tars over anode materials in a fixed bed reactor, and tar effects on SOFC button cells, as shown in Fig. 1. Typical biomass gasification syngas is synthetically generated using pure N_2, H_2, CO, CO_2, and methane (purity > 99.995%, BOC gases) and mixed to the desired partial pressures at a flow rate of 100 ml min^{-1} via a Fideris FCTS GMET mass flow control unit. The gas mixture, excluding CO_2, was passed through a water bath for gas humidification, or directly to a heated line to study the effect that dry gas has on the system. CO_2 was mixed separately downstream of the humidifier to avoid dissolution into the water. Synthetic model tar (benzene) was fed into the heated line via a syringe pump (KD Scientific), producing a tar concentration of 2–15 g Nm^{-3}. A portion of the tar injection line was heated to a temperature slightly above the boiling point of the model tar (85 °C for benzene) to allow vaporization of the tar species into the gas phase and mixing with the incoming syngas. Downstream, depending on the type of experiment, the tar-containing syngas was fed to a heated furnace containing either a quartz tube reactor used to quantify carbon formation on SOFC anode materials, or a SOFC to measure the change in anode performance after exposure to model tar compounds under different operating conditions. The discharge from the reactor or SOFC was sent to a mass spectrometer and/or gas chromatograph for gas stream analysis. Inlet and outlet baseline concentrations were measured using a mass spectrometer while gas flowed through a blank quartz tube reactor or a blank alumina tube similar to that used in the fuel cell test apparatus. The results showed insignificant changes in baseline concentration indicating thermal decomposition of benzene was not occurring.

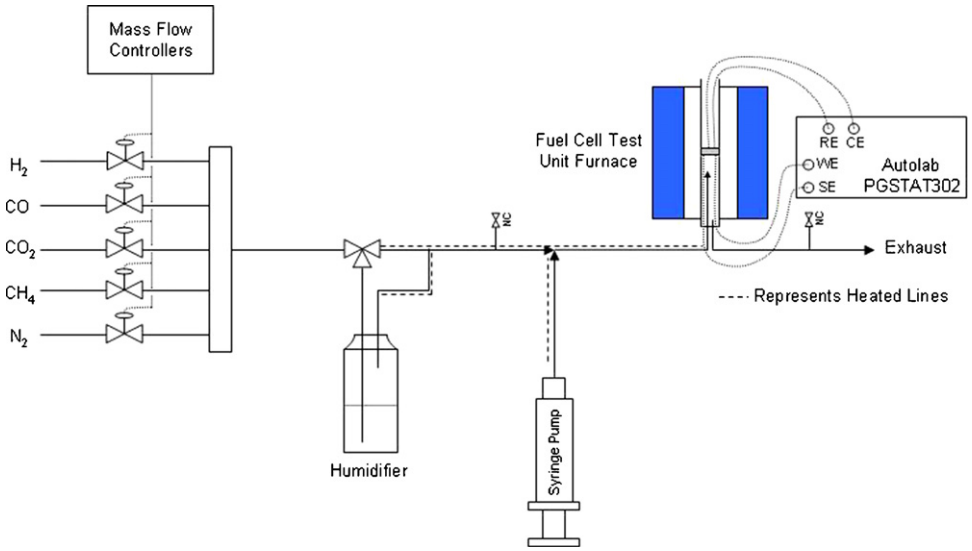

Fig. 1. Schematic illustration of the SOFC test station.

2.2. Fixed bed reactor experiments

A NiO/CGO (gadolinium-doped ceria) powder was derived from an existing screen printable ink sourced from Fuel Cell Materials containing 50% nickel by weight, an average particle size (d_{50}) of 0.34 μm, and a surface area of 7.59 $m^2\,g^{-1}$. The ink was first dried at 250 °C for 2 h and milled to form a fine powder. The powder was then calcined in air at 1300 °C for 3 h and sieved to a particle size of 250 μm.

40 mg of unreduced anode material was lightly compressed between two pieces of quartz wool in the 6 mm OD quartz tube reactor. The material was heated to a typical SOFC operating temperature of 765 °C at a rate of 10 °C min^{-1} in dry nitrogen. Reduction took place by exposing the material at temperature in 2.5% humidified steam and 5% H_2 for 30 min, then increasing to 25% H_2 over a period of 30 min at a flow rate of 50 ml min^{-1}. The sample was then held in 25% H_2 for 30 min. After reduction, flow was increased to 100 ml min^{-1} and the hydrogen concentration changed to the experimental operating conditions of 15% H_2 and the appropriate steam content. Samples were exposed to syngas and benzene model tar for 1 h. The benzene concentration was monitored continuously via an online mass spectrometer (Thermo Fisher Prolab). The downstream gas composition (CO_2, CH_4, and CO) was analyzed by gas chromatography (Varian 3600) after 20 min and 55 min. At the end of the experiment, the reactor was cooled to room temperature in dry 15% H_2 balance N_2.

2.3. Temperature programmed oxidation

Temperature programmed oxidation (TPO) of the sample was done *in situ* to determine the quantity of carbon deposited on the anode material used in fixed bed reactor experiments, assuming total oxidation of carbon to CO_2. Oxidation of the carbon was driven by flowing 80 ml min^{-1} of a 2% O_2 balance argon gas (purity ± 2%, BOC gases) to the reactor with a heating rate of 10 °C min^{-1} from room temperature to 900 °C. A Thermo Fisher Pro Lab mass spectrometer was used to monitor CO_2, CO, O_2, and other minor constituents in the effluent gas stream. A calibration curve was made by diluting a mixture of 1% CO_2 balance argon (purity ± 2%, BOC gases) with argon (purity 99.999%, BOC gases) from 0.05% to 0.5% CO_2 and relating this to the mass intensity as measured by the mass spectrometer.

2.4. SOFC button cell preparation

An electrolyte supported button cell was prepared in order to assess anode performance under varying load and steam conditions in the presence of biomass gasification model tars. Yttria-stabilized zirconia (YSZ) pellets were prepared by pressing 3 g of YSZ (TZ-8Y Zirconia, Tosoh Corporation) powder at 1 tonne pressure for 30 s, before firing at 1450 °C for 5 h at a ramp rate of 5 °C min^{-1}. The pellets were polished using 1200 grit polishing paper to ensure uniform thickness of ~1.4 mm prior to screen printing the anode and cathode on the electrolyte. Nickel oxide cermet ink (50:50 NiO/CGO by weight, FuelCellMaterials, USA) as the anode, and LSM-YSZ (50:50 $(La_{0.80}Sr_{0.20})_{0.98}\ MnO_{3-x}/(Y_2O_3)_{0.08}(ZrO_2)_{0.92}$ by weight, FuelCellMaterials, USA) as the cathode and reference electrode, were screen printed (error of ±125 μm in the placement of electrode geometries) and fired sequentially at 1300 °C and 1150 °C respectively. The anode was a circular disk 1.1 cm in diameter with a cross sectional area of 0.95 cm^2 and the cathode was an identical circular disk, surrounded by a reference electrode with an internal diameter of 17 mm, and an external diameter of 19 mm.

2.5. SOFC performance testing

The fuel cells were tested in a 3-electrode button fuel cell test unit capable of testing fuel cells with diameters of 22–30 mm that was placed within the heated furnace of the test station described above. A description of the button cell test unit can be found in Offer et al., and Mermelstein et al. [1,29]. The cell was taken up to an operating temperature of 765 °C at a ramp rate of 7.5 °C min^{-1} with the anode side exposed to an inert atmosphere. Anode reduction took place by exposing the catalyst at operating temperature in 2.5% humidified steam and 5% H_2 for 30 min, then increasing incrementally to 25% H_2 balance N_2 over a period of 30 min at a flow rate of 50 ml min^{-1}. The sample was then held in 25% H_2 for 30 min. After reduction, flow was increased to 100 ml min^{-1} and the hydrogen concentration changed to the experimental operating conditions of 15% H_2 and the experiment's appropriate steam content. For the electrochemical measurements, an Autolab PGSTAT302 (Eco Chemie BV, The Netherlands) with an FRA module was used as described in Mermelstein et al. [2]. During closed circuit operation, the anode was held galvanostatically at 100–300 mA cm^{-2}, while measuring the anode potential. In this study, anode potential is expressed as the uncorrected potential difference between

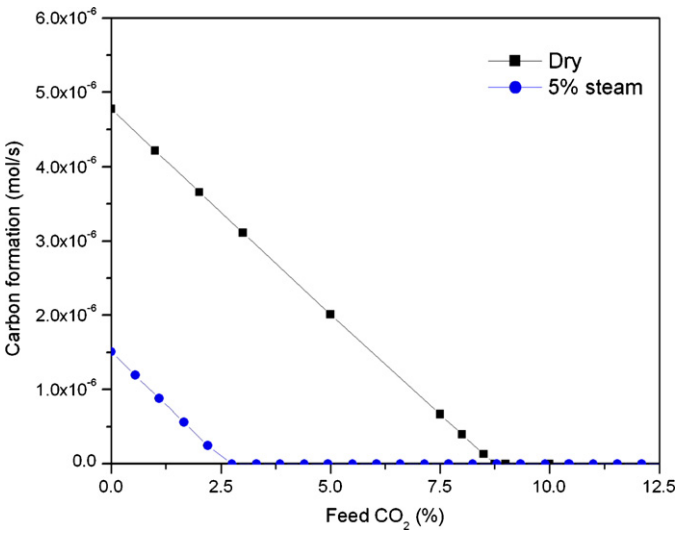

Fig. 2. The effects of CO_2 on suppressing carbon formation in a typical biomass gasification syngas containing 15% H_2, 25% CO, 0–10% CO_2, 2% CH_4 (balance N_2) and 15 g m^{-3} benzene as a model tar in dry and 5% steam conditions calculated by Gibbs free energy minimization at 765 °C using a flow rate of 100 ml min^{-1}.

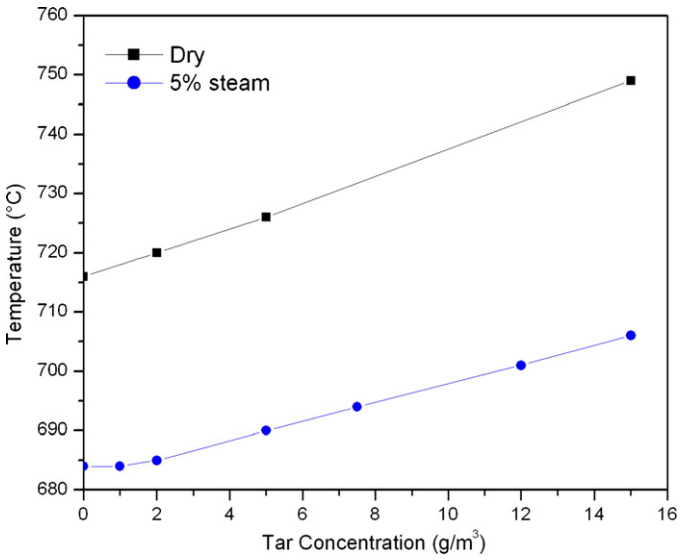

Fig. 3. Threshold temperature dependence of carbon formation in a typical biomass gasification syngas containing 15% H_2, 25% CO, 10% CO_2, 2% CH_4, and up to 15 g m^{-3} benzene as a model tar in 5% steam and dry conditions.

the anode and reference electrode. Autolab FRA and GPES software was used to log and analyze the measurements.

3. Results

3.1. Thermodynamic analysis of boundary conditions for carbon formation for SOFCs operating on biomass gasification syngas containing benzene model tar

In order to operate SOFCs on syngas containing tar compounds, it is important to understand the boundary conditions under which carbon formation can occur under different operating conditions, and where to operate the fuel cell such that carbon formation is suppressed, preventing unwanted anode degradation. Thermodynamic calculations were made using HSC Chemistry software (version 5.11, Outokumpu Research Oy, Finland) [30] with typical syngas containing components of 15% H_2, 25% CO, 0–10% CO_2, 2% CH_4, and 0–5% H_2O and tar levels varying from 0 to 15 g m^{-3} at temperatures from 600 to 800 °C, typical SOFC operating conditions. The elemental composition used for the tar was that of benzene. Using Faraday's law, the amount of oxygen supplied to the anode was calculated to determine the threshold current density to suppress carbon formation arising from tar in a typical biomass gasification syngas operating under different tar loading conditions.

As with steam, sufficient levels of CO_2 are required for dry reforming such that the O/C ratio exceeds the thermodynamic threshold for carbon formation. The calculated effects of CO_2 in the syngas on suppressing carbon formation are shown in Fig. 2 for a dry syngas containing 15% H_2, 25% CO, 2% CH_4, 0–10% CO_2, 15 g m^{-3} benzene with the balance as N_2 at 765 °C, operating at open circuit. The presence of CO_2 in the gas stream leads to a predicted decrease in carbon formation, which is shown to be completely suppressed at CO_2 concentrations exceeding 9% in dry conditions. This was reduced to <3% using 5% steam, typical of the output from a biomass gasifier. This may suggest that an SOFC can operate dry in the presence of tars < 15 g m^{-3} with a typical biomass gasification syngas containing 10% CO_2. However as will be shown in Section 3.2, thermodynamic calculations do not explain the carbon formation observed experimentally when competing reactions of CO_2 and steam reforming are involved. The following does tell us that the additional presence of syngas components prone to decompose into carbon, require higher concentrations of oxidative agents to reduce the effects of carbon formation, whether this be steam, CO_2, or oxygen supplied to the anode under load.

Though calculations show that a typical biomass gasification syngas can operate with tars at temperatures greater than 750 °C, operating at lower temperatures can promote carbon formation. At temperatures up to ~800 °C, tars and hydrocarbon species undergo catalytic decomposition into carbon [21–23]. Carbon formation becomes less thermodynamically stable with increased temperature to a minimum value in the operating range of high temperature SOFCs (~800 °C) [31,32]. The increase in temperature allows for increased oxidation of carbon and higher conversion of the tar associated with increased CO [33]. Higher temperatures can facilitate higher tar conversion [21,33,34], however further increases in temperature to regions > 1000 °C can lead to polymerization of tar compounds into larger PAHs [22,23,35,36]. This causes the condensation of the higher molecular weight products and, inevitably, increased carbon formation. Therefore fuel cell operating temperature plays an important role in determining the likelihood of carbon formation. This is shown in Fig. 3 where the boundary conditions for carbon formation are shown at different operating temperatures in both dry syngas, and syngas containing 5% steam, for different tar concentrations. Thermodynamics predicts carbon formation is likely at temperatures above the lines shown. Hence, as shown in Fig. 3, a typical dry syngas containing 15% H_2, 25% CO, 10% CO_2, and 2% CH_4 at an operating temperature of 765 °C containing 15 g m^{-3} tar, is above the temperature threshold for carbon formation—which sits at ~750 °C. Higher concentrations of tars in the syngas will require higher operating temperatures to convert tar to syngas components rather than carbon. A typical syngas may contain 5% steam, which drops the carbon formation boundary temperature by ~40 °C across all concentrations of tar in the gas stream.

In some cases, the preferred operating temperature for a given SOFC may be in the region where carbon formation is thermodynamically favoured. Under these conditions the fuel cell must be operated above a threshold current density which supplies sufficient oxygen to the anode for complete oxidation of carbon formed from the catalytic decomposition of tar. Faraday's law was used to calculate the moles of oxygen supplied to the anode for a given

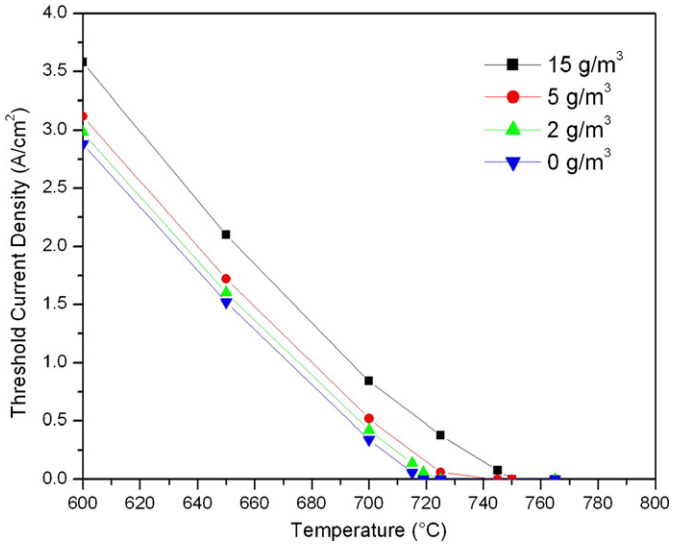

Fig. 4. Calculated threshold current densities as a function of operating temperature to suppress carbon formation in dry conditions for fuel cells operating in 0–15 g m^{-3} benzene as model tar.

current density. Using HSC Chemistry, the threshold current density was determined in dry conditions by calculating the current density at which carbon formation is no longer stable. These values are plotted in Fig. 4 as a function of fuel cell operating temperature and different tar concentrations in a typical biomass gasification syngas. It is clear that a decrease in the tar concentration requires a smaller current density to suppress carbon. However as shown in Fig. 3, carbon formation can occur in the absence of tar at temperatures < 715 °C in dry conditions and <685 °C in 5% steam. In cases of intermediate temperature (IT) SOFCs that operate near 600 °C, threshold current densities are required between 2.8 A cm^{-2} and 3.6 A cm^{-2} for 0 to 15 g m^{-3} tar respectively. These values are below the threshold for re-oxidation of Ni to NiO as shown in Ref. [30], where the Ni–NiO transition exists at a current density of 6.7 A cm^{-2} ($p_{O_2} = 10^{-20}$ bar). However, such high current densities are not readily achievable with current SOFC technology, certainly not without accompanying performance loss over time, as it has been shown that cell degradation increases above 1 A cm^{-2} [37]. Therefore it is evident that commercially available nickel based intermediate temperature SOFCs are not appropriate for operating on the typical biomass gasification syngas described in this paper, regardless of tar concentration, unless high concentrations of steam are supplied to the anode.

3.2. Influence of syngas components on carbon formation from tar over Ni/CGO powder

As previously discussed [30], tar is condensed on the surface of the catalyst with steam until it is completely converted to CO and CO_2. The competition between CO_2 (in the syngas) and steam adsorption for reforming of tar and syngas components could have an effect on syngas conversion and reactions leading to deposition of carbon. Additionally, the condensation of tar on the anode may inhibit reforming of CH_4 and CO in the syngas. Therefore, the formation of carbon on Ni/CGO powder and conversion of benzene exposed to gas containing the following mixtures in Table 1 were compared.

Table 2 shows the conversion of 15 g m^{-3} benzene, fed to the reactor, to carbon on a basis of 102 μl h^{-1} (90 mg/1 h) and carbon deposition as measured by TPO as a function of gas composition. Conversion was highest with H_2 only. This was mainly because the primary chemical reaction involved on the catalyst was benzene steam reforming. CO_2, as discussed above, adsorbs onto the catalyst, competing with steam reforming and therefore it may have had an adverse effect on the catalysts ability to steam reform benzene. Conversion increased slightly with the addition of CO, and further with the addition of CH_4. This may be the result of CO and CH_4 reacting with steam (SMR, WGSR) and CO_2 reformation of CH_4 (reaction (1)) in the gas phase reducing possible inhibiting effects caused by CO_2 adsorption, increasing the catalytic activity for benzene conversion, although further studies would be needed to confirm this. Furthermore, the decomposition of methane at these operating temperatures, as discussed below, is known to form free radicals and products that interact with benzene to form larger PAHs [27,28,38–46] resulting in an increase in benzene conversion.

Table 1
Syngas mixtures.[a]

(1)	15% H_2
(2)	15% H_2, 10% CO_2
(3)	15% H_2, 10% CO_2, 25% CO
(4)	15% H_2, 10% CO_2, 25% CO, 2% CH_4

[a] All mixtures contain 5% steam balance N_2.

Fig. 5 shows the evolution of CO_2 during TPO from the oxidation of carbon formed on 36 mg Ni/CGO powder exposed to the syngas mixtures described in Table 1, with the amount of carbon formed, as measured by TPO, in Table 2. For each syngas mixture tested in Table 1, carbon formation was not detected in the absence of tar. TPO results in Fig. 5 show the presence of one main peak at ~680–700 °C for each syngas composition, indicating the presence of amorphous char type carbon. As shown in Table 2, carbon is decreased with the addition of CO_2 to the syngas in mixture (2).

The addition of CO in mixture (3) led to an increase in carbon formation. Although there is the possibility that the presence of tar inhibits the WGSR [47,48], leading to CO disproportionation increasing carbon formation, the Boudouard equilibrium at high temperatures is shifted to the left for the reaction $2CO \leftrightarrow CO_2 + C$ [49] with maximum carbon formation peaking at 500 °C on Ni/YSZ anode material [50]. Therefore the increase in carbon may be attributed to the reduction in steam available for reforming of benzene as a result of the WGS reaction.

As in the case of CO, steam reforming of CH_4 added to the syngas may have contributed to a decrease in the steam available for reforming of benzene, increasing carbon formation. Additionally, the large increase in carbon formation from the addition of CH_4 is both characteristic of CH_4 decomposition at these operating temperatures and of PAH polymerization and condensation as soot resulting from the interaction of CH_4 decomposition products and benzene [27,28,38–46]. CH_4 pyrolysis has been extensively studied with much attention drawn to acetylene selectivity, which is maximized in H_2 environments such as those used in these experiments [39]. Acetylene has been considered as a principal intermediate for

Table 2
Measured carbon deposition from TPO on 36 mg Ni/CGO powder (dp > 250 μm) and conversion of 15 g m^{-3} benzene fed to the reactor operating at 765 °C in syngas mixtures of H_2, CO_2, CO, and/or CH_4 as described in Table 1.

Gas mixture	Carbon deposited (mg)	Benzene conversion	Benzene conversion to carbon[a]
(1)	0.459	45%	0.51%
(2)	0.083	23%	0.09%
(3)	0.672	26%	0.75%
(4)	3.5	32%	3.9%

[a]Note that CH_4 and CO can contribute to carbon formation and it is not known how much carbon formed from benzene alone. Difficulties exist in predicting the rate of carbon formation for hydrocarbon pyrolysis and CO disproportionation as it strongly depends on thermodynamic and kinetic aspects of the reactions and system operating conditions such as gas composition [51].

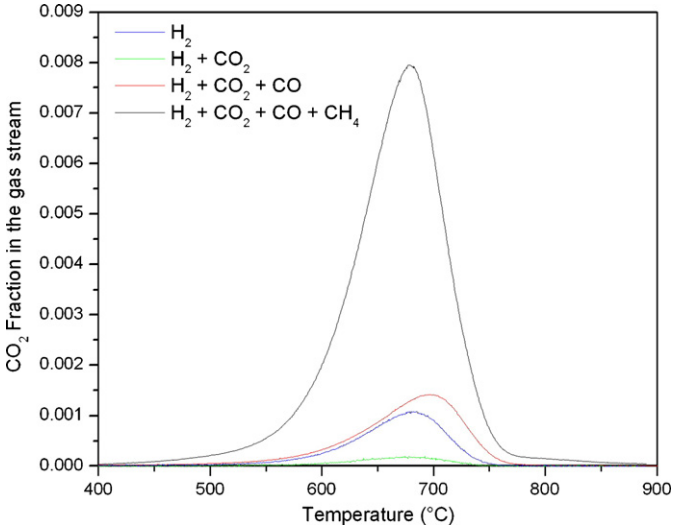

Fig. 5. CO_2 fraction in the gas as a function of temperature measured by TPO of 36 mg Ni/CGO powder (dp > 250 μm) exposed to syngas containing 15% H_2, 10% CO_2, 25% CO, and/or 2% CH_4 and 15 g m^{-3} benzene.

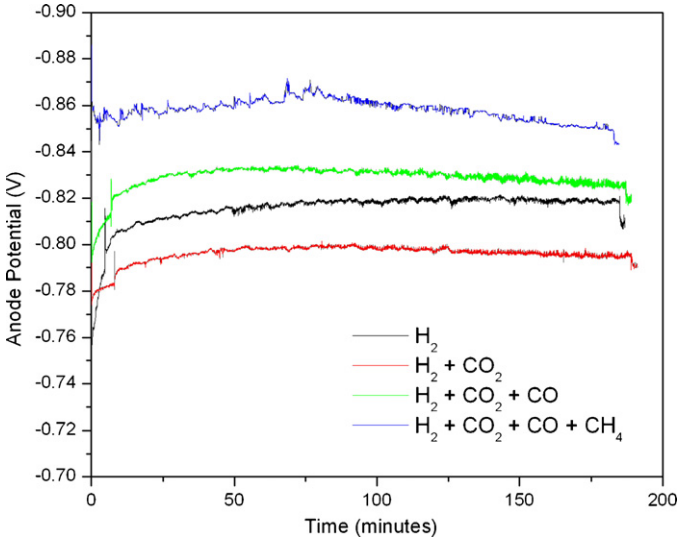

Fig. 6. Change in Ni/CGO anode potential operating at 100 mA cm^{-2} for 3 h in the presence of 15 g m^{-3} benzene model tar in syngas compositions containing 15% H_2, 10% CO_2, 25% CO, and/or 2% CH_4 as described in Table 1 with 5% steam 765 °C.

growth of small PAHs [38,40] through the mechanism proposed by Frenklach [40]. Growth of benzene to larger PAHs thus involves the addition of C_2 and C_3 to PAH radicals and PAH–PAH radical recombination [27]. The resulting carbon therefore deposits on the catalyst and is detected in the region of amorphous char carbon during TPO measurements.

3.3. Time dependent behaviour of SOFC anodes operating on tar laden biomass gasification syngas

It has been shown that the effect of carbon on the performance of the anode can be reduced by means of steam reforming [2,30], CO_2 reforming, and partial oxidation via oxygen ion transport from increased current density [2]. However the impact of tars exposed to the anode in different compositions of gasification syngas over periods of several hours is not well known. 2–15 g m^{-3} benzene as model tar was therefore fed to the anode of separate fuel cells for 3 h with the gas compositions discussed in Table 1, operating at a current density of 100–300 mA cm^{-2} in 5% humidified steam.

The trends over time for each gas composition (1–4) operating at 100 mA cm^{-2} are shown in Fig. 6. Separate fuel cells were used in this study for each current density, and variation in the screen printing of the electrodes and connections within the fuel cell test station can therefore affect the anode potential under load. However there is a clear trend in that the addition of CO and CH_4 increased the anode potential, indicating higher anode performance. This is consistent with results previously described in Ref. [2] where the exposure to tars outside thermodynamic limits for carbon formation showed improved anode performance over 30 min exposures. However at longer times the anode began to degrade, with evidence of a decline in anode potential. The maximum time the anode was able to operate in its corresponding syngas before degradation occurred is described in Table 3. The syngas containing only H_2, N_2, steam, and tar operated the longest, being ~140 min before degradation occurred. The fuel cells operating in syngas containing CO_2, CO, and/or CH_4 were only able to operate for ~75 min before anode performance began to degrade. The degradation in anode potential at 100 mA cm^{-2} increased with the subsequent addition of CO_2, CO, and CH_4, as shown in Table 3. The amount of degradation in anode performance can also be related to the amount of carbon formed on the anode, as shown in the image in Fig. 7(A). Here, only a small dusting of carbon is seen on the surface of the anode exposed to just H_2 and tar. The addition of CO_2 created a ring like formation of carbon around the circumference of the anode. The addition of CO to the syngas led to moderate carbon formation on a majority of the anode surface. Carbon formation and anode degradation was most severe with the addition of 2% CH_4. A separate fuel cell was operated on syngas containing all components in these conditions without tar, and carbon formation was not observed. Similar trends in these results occurred with the exposure of each syngas composition, with and without tar, over Ni/CGO powder as described earlier. This shows that carbon formation becomes even more likely as we move towards more technologically relevant gasifier compositions.

As shown in Fig. 7(A), biomass gasification tar concentrations of 15 g m^{-3} are severely damaging under moderate current densities of 100 mA cm^{-2} for each of the syngas compositions tested. Therefore similar Ni/CGO anodes were subjected to 2–15 g m^{-3} benzene model tar at a higher current density of 300 mA cm^{-2} (Fig. 8). The higher current density was used to determine if the fuel cell could operate without severe damage at a high tar loading of 15 g m^{-3}, and to determine what levels of tar the fuel cell might withstand under longer term operation. As shown in Fig. 8, the anode potentials were quite low, in the range of −0.25 to −0.35 V for each anode, reflecting the relatively high polarization resistance of the anodes tested. Downstream gas analysis showed that conversion of benzene was negligible (<5%). It can be seen in all three cases that the anode showed a rapid initial decrease in performance, followed by a much slower decrease over the duration of the experiment, tending towards stable operation, though at a much higher overpotential.

Visual inspection of the fuel cells in Fig. 7(B) and the SEM image in Fig. 9 shows a faint dusting of carbon on the surface of the anode

Table 3
Maximum time the fuel cell was able to operate at 100 mA cm^{-2} before the anode began to degrade, together with the anode potential degradation from its peak performance during exposure to 15 g m^{-3} tar in syngas compositions containing 15% H_2, 10% CO_2, 25% CO, and/or 2% CH_4 as described in Table 1 with 5% steam at 765 °C.

Gas mixture	Max time before anode degradation (min)	Anode potential degradation (%)
(1)	143	0.3
(2)	81	0.8
(3)	72	1.13
(4)	72	1.85

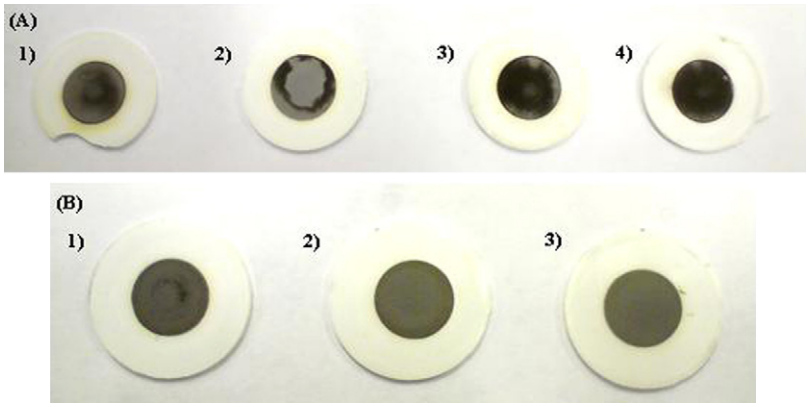

Fig. 7. Images of carbon formation on Ni/CGO anodes after (A), 3 h exposure to 15 g m^{-3} benzene model in syngas compositions of (1) 15% H_2, (2) 15% H_2 + 10% CO_2, (3) 15% H_2 + 10% CO_2 + 25% CO, (4) 15% H_2 + 10% CO_2 + 25% CO + 2% CH_4 in 5% humidified steam operating at 100 mA cm^{-2} and (B), 3 h exposure to (1) 15 g m^{-3}, (2) 5 g m^{-3}, (3) 2 g m^{-3} benzene model in syngas composition of 15% H_2 + 10% CO_2 + 25% CO + 2% CH_4 in 5% humidified steam operating at 300 mA cm^{-2} and 765 °C.

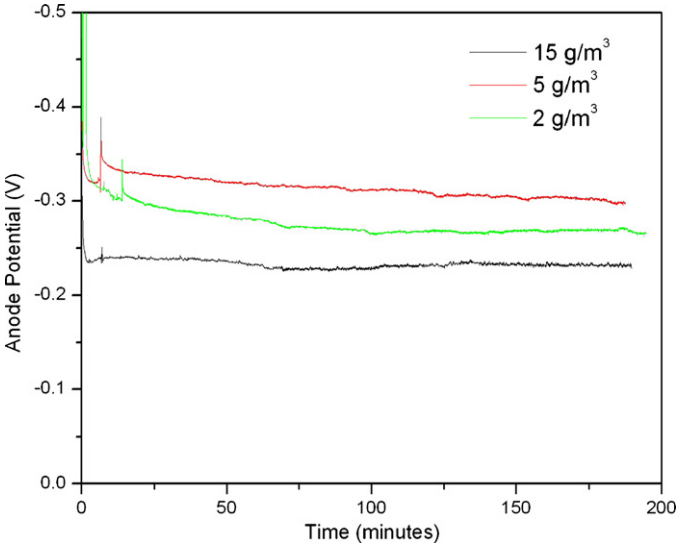

Fig. 8. Change in Ni/CGO anode potential operating at 300 mA cm^{-2} for 3 h in the presence of 2–15 g m^{-3} benzene model tar in syngas compositions containing 15% H_2, 10% CO_2, 25% CO, and 2% CH_4.

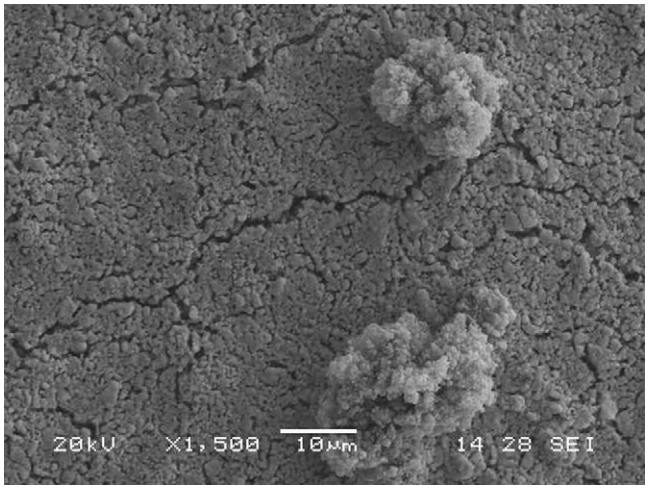

Fig. 9. SEM micrographs showing agglomerates of carbon sitting on the surface of the Ni/CGO anode exposed to 15 g m^{-3} benzene as model tar in a typical gasification syngas for 3 h operating at 300 mA cm^{-2} and 765 °C.

after exposure to 15 g m^{-3} benzene model tar. The microstructure of the anode was not damaged and small agglomerates of carbon were seen on its surface. Carbon formation was not present after exposure to 2 and 5 g m^{-3} benzene model tar. Differences before and after anode polarization were found to be negligible, however there was a slight increase in anode potential after exposure to 15 g m^{-3} tar. This may be a result of microstructural changes occurring from very limited deposits of carbon on the surface of the anode affecting the conductivity, but not the electrochemical response of the anode [2].

4. Conclusions

An experimental study has been made on the effect of gasification tar on the operation and durability of high temperature SOFC anodes in typical biomass gasification syngas. Generally, steam and CO_2 work in conjunction to reduce carbon formation. However the competition between CO_2 and steam adsorption on the catalyst with the tar, may have an adverse effect on tar conversion.

The addition of CO and CH_4 increased the amount of carbon deposited on the surface of both the anode powder and the SOFC, most significantly with the addition of CH_4. It is believed that the additional carbon formed from CO was due to a reduction in steam available for benzene reforming as a result of the WGS reaction. The increase in carbon from CH_4 may be attributed to CH_4 decomposition to carbon and the interaction of CH_4 decomposition products with benzene free radicals to form higher molecular weight PAHs that condense on the anode material as amorphous char type carbon.

Operation of the fuel cell at 100 mA cm^{-2} showed that the fuel cell could be operated in the presence of 15 g m^{-3} tar in H_2 without measured degradation over 3 h, however carbon deposition was present on the anode in notable amounts, indicating that degradation would be expected after longer times. The subsequent addition of each syngas component, 10% CO_2, 25% CO, and 2% CH_4 caused increased degradation of the anode, whereas the absence of tars in the syngas did not lead to carbon formation. This shows that carbon formation becomes more likely as we move towards more technologically relevant gasification mixtures.

Operating the fuel cell at 300 mA cm^{-2} over 3 h in a typical biomass gasification syngas with <5 g m^{-3} tars did not show the formation of carbon, and degradation of the anode may have been associated with the associated higher anode over-potential. Some minor carbon deposition did occur when the fuel cell was exposed to 15 g m^{-3} tar. However, this did not have an effect on the electrochemical response of the fuel cell, although over long term

operation, tar concentrations of the levels used in this study would not be considered acceptable for SOFC anodes.

References

[1] J. Mermelstein, M. Millan, N.P. Brandon, Chemical Engineering Science 64 (2009) 492–500.
[2] J. Mermelstein, M. Millan, N. Brandon, Journal of Power Sources 195 (2009) 1657–1666.
[3] B.S Liu, C.T. Au, Applied Catalysis A: General 244 (2003) 181–195.
[4] K.J. Puolakka, S. Juutilainen, A.O.I. Krause, Catalysis Today 115 (2006) 217–221.
[5] D. Sutton, S.M. Parle, J.R.H. Ross, Fuel Processing Technology 75 (2002) 45–53.
[6] M. Wisniewski, A. Boréave, P. Gélin, Catalysis Communications 6 (2005) 596–600.
[7] S. Assabumrungrat, N. Laosiripojana, P. Piroonlerkgul, Journal of Power Sources 159 (2006) 1274–1282.
[8] J.H. Edwards, A.M. Maitra, Fuel Processing Technology 42 (1995) 269–289.
[9] N. Laosiripojana, W. Sutthisripok, S. Assabumrungrat, Chemical Engineering Journal 112 (2005) 13–22.
[10] J.M. Ginsburg, J. Pina, T. El Solh, H.I. de Lasa, Industrial & Engineering Chemistry Research 44 (2005) 4846–4854.
[11] D.J. Moon, J.W. Ryu, Catalysis Today 87 (2003) 255–264.
[12] Y. Shiratori, T. Oshima, K. Sasaki, International Journal of Hydrogen Energy 33 (2008) 6316–6321.
[13] C.M. Finnerty, N.J. Coe, R.H. Cunningham, R.M. Ormerod, Catalysis Today 46 (1998) 137–145.
[14] K.M. Walters, A.M. Dean, H. Zhu, R.J. Kee, Journal of Power Sources 123 (2003) 182–189.
[15] J.H. Koh, B.S. Kang, H.C. Lim, Y.-S. Yoo, Electrochemical and Solid-State Letters 4 (2) (2001) A12–A15.
[16] D. Singh, E. Hernandez-Pacheco, P.N. Hutton, N. Patel, M.D. Mann, Journal of Power Sources 142 (2005) 194–199.
[17] V.R. Choudhary, B.S. Uphade, A.S. Mamman, Applied Catalysis A: General 168 (1998) 33–46.
[18] J.R. Rostrup-Nielsen, J.H.B. Hansen, Journal of Catalysis 144 (1993) 38–49.
[19] B. Frank, F.C. Jentoft, H. Soerijanto, J. Kröhnert, R. Schlögl, R. Schomäcker, Journal of Catalysis 246 (2007) 177–192.
[20] N. Laosiripojana, S.K. Rajesh, W. Singhto, T. Palikanon, S. Pengyong, The Third Regional Conference on Energy Technology towards a Clean Environment "Sustainable Energy and Environment (SEE)", Thailand, December, 2004, pp. 129–133.
[21] J. Han, H. Kim, Renewable and Sustainable Energy Reviews 12 (2008) 397–416.
[22] A.P. Rudenko, A.A. Balandin, S.Y. Kachan, Russian Chemical Bulletin 9 (1960) 917–923.
[23] G Stegner, A.A. Balandin, A.P. Rudenko, Russian Chemical Bulletin 8 (1959) 1811–1818.
[24] M.J. Antal, Industrial & Engineering Chemistry Product Research and Development 22 (2002) 366–375.
[25] J.J. Strohm, J. Zheng, C. Song, Preprints of Symposia—American Chemical Society, Division of Petroleum Chemistry 48 (2003) 931–933.
[26] H. He, J.M. Hill, Applied Catalysis A: General 317 (2007) 284–292.
[27] H. Richter, J.B. Howard, Progress in Energy and Combustion Science 26 (2000) 565–608.
[28] J.F. Roesler, S. Martinot, C.S. McEnally, L.D. Pfefferle, J.L. Delfau, C. Vovelle, Combustion and Flame 134 (2003) 249–260.
[29] G.J. Offer, P. Shearing, J.I. Golbert, D.J.L. Brett, A. Atkinson, N.P. Brandon, Electrochimica Acta 53 (2008) 7614–7621.
[30] J. Mermelstein, N.P. Brandon, M. Millan, Energy and Fuels 23 (2009) 5042–5048.
[31] J. Wu, Y. Fang, H. Peng, Y. Wang, Fuel Processing Technology 86 (2004) 261–266.
[32] I.V. Yentekakis, T. Papadam, G. Goula, Solid State Ionics 179 (2008) 1521–1525.
[33] A. Jess, Chemical Engineering and Processing 35 (1996) 487–494.
[34] T.A. Milne, R.J. Evans, Biomass Gasifier "Tars": Their Nature, Formation, and Conversion, National Renewable Energy Lab, 1998, NREL/TP-570-25357.
[35] Y. Cao, Y. Wang, J.T. Riley, W.-P. Pan, Fuel Processing Technology 87 (2006) 343–353.
[36] D.C. Elliot, in: E.J. Soltes, T.A. Milne (Eds.), Relation of Reaction Time and Temperature to Chemical Composition of Pyrolysis Oils, ACS Symposium Series 376, Pyrolysis Oils from Biomass, 1987, Denver, CO, April.
[37] N. Christiansen, J.B. Hansen, H. Holm-Larsen, S. Linderoth, P.H. Larsen, P.V. Hendriksen, M. Mogensen, Fuel Cells Bulletin 2006 (2006) 12–15.
[38] J. Canes, S. Valin, P. Castelli, S. Thiery, C. Dupont, M. Petit, Proceedings of the Advanced Atmospheric Aerosol Symposium, 2008, pp. 1–9.
[39] A. Dufour, S. Valin, P. Castelli, S.B. Thiery, G. Boissonnet, A. Zoulalian, P.-A. Glaude, Industrial & Engineering Chemistry Research 48 (2009) 6564–6572.
[40] M. Frenklach, Physical Chemistry Chemical Physics 4 (2002) 2028–2037.
[41] H. Li, A. Goldbach, W. Li, H. Xu, Journal of Membrane Science 324 (2008) 95–101.
[42] H. Richter, T.G. Benish, O.A. Mazyar, W.H. Green, J.B. Howard, Proceedings of the Combustion Institute 28 (2000) 2609–2618.
[43] H. Richter, S. Granata, W.H. Green, J.B. Howard, Proceedings of the Combustion Institute 30 (2005) 1397–1405.
[44] J.F. Roesler, M.A.d. Tessan, X. Montagne, Chemosphere 42 (2001) 823–826.
[45] M.S. Skjøth-Rasmussen, P. Glarborg, M. Østberg, J.T. Johannessen, H. Livbjerg, A.D. Jensen, T.S. Christensen, Combustion and Flame 136 (2004) 91–128.
[46] M. Weissman, S.W. Benson, Progress in Energy and Combustion Science 15 (1989) 273–285.
[47] P. McKendry, Bioresource Technology 83 (2002) 55–63.
[48] M. Ni, D.Y.C. Leung, M.K.H. Leung, K. Sumathy, Fuel Processing Technology 87 (2006) 461–472.
[49] Z. Wang, W. Weng, K. Cheng, P. Du, G. Shen, G. Han, Journal of Power Sources 179 (2008) 541–546.
[50] B. Novosel, M. Avsec, J. Macek, Materials and Technology 42 (2008) 51–57.
[51] S. Presto, A. Barbucci, M. Carpanese, M. Viviani, R. Marazza, Journal of Applied Electrochemistry (2009), doi:10.1007/s10800-009-9857-7.